



Published in final edited form as:

*J Magn Reson.* 2014 September ; 246: 31–35. doi:10.1016/j.jmr.2014.06.020.

## Accurate scoring of non-uniform sampling schemes for quantitative NMR

Phillip C. Aoto, R. Bryn Fenwick, Gerard J. A. Kroon, and Peter E. Wright\*

Department of Integrative Structural and Computational Biology and the Skaggs Institute for Chemical Biology, The Scripps Research Institute, La Jolla, CA 92037

### Abstract

Non-uniform sampling (NUS) in NMR spectroscopy is a recognized and powerful tool to minimize acquisition time. Recent advances in reconstruction methodologies are paving the way for the use of NUS in quantitative applications, where accurate measurement of peak intensities is crucial. The presence or absence of NUS artifacts in reconstructed spectra ultimately determines the success of NUS in quantitative NMR. The quality of reconstructed spectra from NUS acquired data is dependent upon the quality of the sampling scheme. Here we demonstrate that the best performing sampling schemes make up a very small percentage of the total randomly generated schemes. A scoring method is found to accurately predict the quantitative similarity between reconstructed NUS spectra and those of fully sampled spectra. We present an easy-to-use protocol to batch generate and rank optimal Poisson-gap NUS schedules for use with 2D NMR with minimized noise and accurate signal reproduction, without the need for the creation of synthetic spectra.

### Keywords

non-uniform sampling; NMR; quantitative NUS; NUS scoring function; optimal NUS; Poisson-gap sampling

### 1. Introduction

Non-uniform sampling (NUS) affords significant time-savings in acquisition of NMR data by sampling only a percentage of the indirect time domain, extending the range of NMR to highly multidimensional experiments as well as to protein systems with poor signal-to-noise [1–3]. Recent advances in reconstruction and sampling methods for NUS have focused on increasing sensitivity and resolution over reduced or similar measurement times [1,4]. The utilization of the time savings and sensitivity gains of NUS in quantitative NMR experiments, such as CPMG relaxation dispersion,  $T_1$ ,  $T_2$ , and  $T_{1\rho}$  relaxation, and

© 2014 Elsevier Inc. All rights reserved.

Correspondence to: wright@scripps.edu, +1 (858) 784-9721.

**Publisher's Disclaimer:** This is a PDF file of an unedited manuscript that has been accepted for publication. As a service to our customers we are providing this early version of the manuscript. The manuscript will undergo copyediting, typesetting, and review of the resulting proof before it is published in its final citable form. Please note that during the production process errors may be discovered which could affect the content, and all legal disclaimers that apply to the journal pertain.

heteronuclear NOE experiments, are only now starting to be explored [5]. Artifacts from the reconstruction and the sampling scheme can be tolerated for multidimensional qualitative experiments, but are detrimental in quantitative NMR experiments that rely entirely on measured peak intensities. Many NUS reconstruction methods have been developed [6–11], with a few, such as compressed sensing, SIFT (Spectroscopy by Integration of Frequency and Time domain information), and CLEAN promising the greatest accuracy of intensity reproduction over a high dynamic range [12–17].

The NUS scheme is a crucial determinant of the reconstructed spectral quality. Sensitivity can be increased by adding a forward weight to the data collection so that a higher percentage of the early (strongest) portion of the exponential decaying time-domain signal is collected [2,18,19]. On the other hand, randomization of the sampling scheme helps prevent systematic violation of the Nyquist sampling theorem and is an important factor in minimizing spectral artifacts [18,20–22]. Many sampling methodologies balance the requirement for randomization and the desire for forward weighted collection [1,2,21–23]. Still, it has been found that the quality of a sampling scheme depends heavily on the random seed used to create the scheme [1,24]. Some methods, such as sine-weighted Poisson-gap sampling [1,24], have demonstrated a weaker dependence on the random seed compared to other random NUS methods, such as complete random, hybrid uniform/non-uniform, and exponentially weighted random sampling. Still, an increase in dependence on the random seed in reconstruction quality with Poisson gap schemes has been suggested when a higher percentage of points or lower number of reconstructed increments are used, since the points available for selection become limited [1]. Other sampling methods make use of a deterministic schedule, eliminating the need for a random seed altogether [25]. However, these deterministic schedules require knowledge of the spectra prior to NUS data collection and therefore are not suited for all situations. It has also been suggested that random sampling schemes are more robust and only slightly less sensitive than knowledge based sampling [26].

## 2. Performance of Poisson-gap sampling schemes

We chose to use the sinusoidal weighted Poisson-gap sampling method to generate schemes for quantitative NMR [24]. In order to evaluate the performance of sinusoidal weighted Poisson gap sampling, with increments routinely used in quantitative 2D NMR, we tested a variety of conditions varying in sampling completeness (%NUS) and total number of increments. For a given Poisson-gap sampling condition (%NUS and total increments) 2,000 to 10,000 schemes, from code derived from reference 24, were generated (see details in SI). Various synthetic 2D  $^{15}\text{N}$  HSQC and  $^{13}\text{C}$  HSQC spectra were created with linewidths and number of resonances approximating an 18kDa protein. Discrete Fourier transform (DFT) of non-reconstructed data and non-convex iterative re-weighted least squares compressed sensing reconstruction [12,27] were used with the NUS synthetic data to create 2D spectra with the programs MDDNMR and NMRPipe [8,12,28]. Following reconstruction, identical processing was performed on all data. Minimal apodization, by a cosine window function, was utilized in the reconstructed dimension. The quality of each reconstructed spectrum was measured by taking the total RMS difference between the full linearly sampled synthetic spectrum containing no noise and the NUS reconstructed spectrum. The RMS calculation

was performed with the NMRPipe software package [28]. The resulting RMS can be considered a measure of the total sampling artifacts and accuracy of peak reconstruction because it is sensitive to peak position, peak shape, and peak intensity in the reconstructed spectrum.

Using 60% NUS with a typical number of increments in the indirect dimension (e.g. 128 complex pairs) we found that a strong dependence of RMS on random seed in Poisson-gap sampling emerges (Figure 1). Examples of the worst and best RMS reconstructed spectra are shown in Figures 1a–b, respectively. The severity of the sampling artifacts is also demonstrated by the difference spectra between the reconstructed and uniformly sampled spectra for the best and worst RMS schemes (SI). A very small percentage of schemes give a greater than 2-fold improvement in reconstruction compared to the worst scheme. For example, we found that only 0.05% (40/10,000) of the schemes lead to low artifact intensity in the best 5% of measured RMS (Figure 1c -histogram). This necessitates the generation and evaluation of a very large number of schemes ( $\gg 200$ ) in order to obtain at least one optimal scheme. It is worth noting that the histogram for the Poisson-gap generated schemes in Figure 1c is skewed towards ‘good’ RMS, in agreement with reference 24, which found that as opposed to other random-seed based schemes the Poisson-gap method produces a large percentage of schemes that have very little variation in performance. The loss of some of this performance for data sets with fewer total reconstructed complex pairs ( $< 1024$ ) as discussed in reference 1 is also apparent here.

### 3. Current NUS scoring functions

We next examined the best way to select an optimal sampling schedule, without batch reconstruction. Various methods to score NUS schemes prior to data collection have been given [1,29,30]. These make use of the point-spread-function (PSF) of the sampling scheme in some way. The PSF is the frequency domain response of the sampling schedule. Therefore the PSF is an indicator of the quality of an NUS schedule. A comparison of current NUS scoring functions was performed using the aforementioned synthetic  $^{15}\text{N}$ -HSQC-like dataset. A commonly cited scoring function, the PSF ratio [2, 29], is expected to predict with the lowest ratio the scheme that yields the lowest artifacts. However, this was not observed in our simulations. In 10,000 sampling schemes the PSF ratio was unable to predict the amplitude of reconstruction artifacts (RMS) yielding a correlation coefficient of  $\rho = 0.09$  (Figure 1c). Another popular scoring method makes use of the difference or  $l_2$  norm between NUS and fully sampled signal [1]. To obtain an  $l_2$  norm, fully sampled and NUS synthetic 2D spectra containing 4 to 20 randomly positioned cross peaks were compared, similarly to the RMS calculation. Not surprisingly, the  $l_2$  norm method was able to predict the propensity of a sampling scheme to produce artifacts in a 2D experiment ( $\rho = 0.87$ ) (Figure 1d). However, the  $l_2$  norm requires reconstruction of a synthetic spectrum for each sampling scheme, which is time-consuming and not a straightforward task. Thus there is a need for a robust, fast, and easy to use scoring method.

#### 4. A quantitative NUS scoring method

In order to empirically score Poisson-gap sampling schemes we first considered the two conflicting characteristics that must be balanced to obtain a spectrum with high sensitivity and minimal artifacts. These two elements are 1) forward weighted collection to increase sensitivity and 2) random selection of points to reduce spectral artifacts. A score was developed to determine how well a sampling scheme follows the desired weight of Poisson-gap sampling. This was based on the probability mass function (PMF) of a sinusoidal weighted Poisson gap distribution:

$$\beta_{PMF} = (\lambda^k / k!) e^{-\lambda}$$

which gives the probability of a gap,  $k$ , between increments (e.g. between two consecutive points,  $k=1$ ) and where  $\lambda$  depends on a sinusoidal weight of the increment position defined in reference 24 as:

$$\lambda = a \sin \theta$$

where  $a$  is the weighting factor and  $\theta$  varies from 0 to  $\pi/2$  as more increments are selected. A score to account for randomness was also designed. This takes the summation of a two point moving average of the point-spread function:

$$\beta_{PSF} = \sum_i [PSF(i) + PSF(i+1)] / 2$$

where  $PSF(i)$  is the real point spread function of the sampling schedule at frequency  $i$ . The zero-frequency peak is omitted in the summation so that only PSF artifacts contribute to the score. We found that by de-weighting the first and last points of the PSF, or the frequencies closest and farthest from the reconstructed peak, the  $\beta_{score}$  became a more accurate predictor of the quality of the sampling scheme. An empirically derived combination of the 2 scores was found to give the best results:

$$\beta_{score} = \beta_{PMF} w_{PMF} + \beta_{PSF} w_{PSF}$$

where  $\beta_{score}$  is the score for the NUS scheme and  $w_{PSF}$  and  $w_{PMF}$  are empirically derived weights.  $w_{PSF} = 2/3$  and  $w_{PMF} = 2^{-64/td}$ , where  $td$  is the total number of complex pairs in the final reconstructed spectrum. Thus, as a higher number of complex pairs are collected the  $\beta_{PMF}$  score becomes a better predictor of sampling scheme quality. The value of 64 was chosen because, in our experience, this is near the lower limit of complex pairs normally acquired. It is worth reemphasizing that the weights given to each score are completely empirical, but the overall score as shown below performs very well across a wide range of sampling conditions.

In 10,000 sampling schemes under the same conditions as above we found a very good correlation between our NUS score and the RMS of reconstructed spectra (with a correlation

coefficient of  $\rho = 0.66$ ) (Figure 2a). The top 10 schemes predicted by the scoring function are in the top 20% of the sampling schedules. In addition, within the top 10 there are schemes that lie within the best 0.03% of all 10,000 sampling schedules, with respect to RMS. To test whether there is a scoring bias towards a specific spectrum, a synthetic  $^{13}\text{C}$  HSQC spectrum was also reconstructed from 10,000 NUS datasets and found to have a similar correlation ( $\rho = 0.77$ ) to the original results (Figure 2b).

Since compressed sensing reconstruction used in the examples above may have introduced bias into our empirical NUS scoring method, we compared the score to spectra processed with DFT (Figure 2a). As opposed to compressed sensing, where missing points are reconstructed, in DFT points that have not been collected are set to 0. This exaggerates sampling artifacts and reflects the convolution of the PSF and uniformly sampled spectra. Since the sampling score here has contributions from the PSF it is not surprising that there is a good correlation between the RMS and NUS score of the DFT spectra. This suggests that the scoring function may be generally applicable to other statistical reconstruction methods, such as those in reference 11.

Next, the NUS scoring method was tested for any dependence on the parameters used to generate the sampling schedules. Schemes at 30% and 60% NUS at both 256 and 512 total linear increments were examined and found to give good correlations (ranging from  $\rho = 0.62$  to  $\rho = 0.87$ ) between score and RMS (Figure 2c,d). These results suggest that our NUS scoring method is mostly independent of NUS parameters.

We also reconstructed real NMR data to further investigate the generality of our scoring method. The  $^1\text{H}$ - $^{15}\text{N}$  TROSY spectrum of a 43kDa protein (the MAP kinase p38 $\gamma$ ) was reconstructed using 2,000 sampling schemes at 60% NUS. Again a good correlation between score and RMS was found ( $\rho = 0.80$ , SI). Finally, application of scoring methods to quantitative NMR requires identification of schemes that give accurate reconstructed peak intensities over a high dynamic range. Our scoring method should also predict the accuracy of peak reconstruction since the RMS measurement partially reflects this attribute. Indeed, we found this to be the case. Peak intensities were measured [31] for the ten best and worst scored schemes at 60% NUS for the 18kDa globular protein dihydrofolate reductase (DHFR), the 43kDa kinase p38 $\gamma$ , and the globular 17kDa protein apomyoglobin. The accuracy of the intensity reconstructions for the ten best and ten worst scoring sampling schemes for these proteins are shown in Figures 3a–c. The best schemes accurately reproduce the intensities of the uniformly sampled spectra for all 3 proteins, with higher fidelity than the worst schemes. Resonances closer to the noise (e.g.  $<4\times$  the noise) show greater susceptibility to be poorly reconstructed by the worst schemes. The 10 best schemes have a greater number of resonances that are reconstructed with close to 0% error and a narrower distribution of errors than the 10 worst schemes (Figure 3d–f)

## 5. Conclusions

We have developed software that generates a large number of schemes based on user input for the desired percent NUS and weight. The software scores the schemes and presents the user with the top 10 scores. The highest scoring schemes will likely perform in the top 20%

of all schemes generated in terms of minimal sampling artifacts and optimal peak reconstruction. The method does not require any synthetic reconstruction to obtain scores, however the top-10 scores, which represent generally optimal schemes, may be tested using the RMS method described above with fully sampled spectra of the protein of interest to find the scheme within the top-10 scores that is best suited for each particular case. Although we have presented the scoring function in the context of the Poisson-gap sampling the same basic concepts are likely applicable for choosing optimal schemes from other random-seed generated sampling methods, for example with relaxation-matched exponential sampling. The software, written in C++ and python, has been tested on hardware running Linux and Mac OS X and is available online for download (<http://www.scripps.edu/wright>).

## Supplementary Material

Refer to Web version on PubMed Central for supplementary material.

## Acknowledgments

The authors would like to thank David Oyen for NMR samples and helpful discussions. PEW is supported by grant GM75995 from the National Institutes of Health and by the Skaggs Institute for Chemical Biology.

## References

1. Hyberts SG, Arthanari H, Wagner G. Applications of non-uniform sampling and processing. *Top Curr Chem*. 2012; 316:125. [PubMed: 21796515]
2. Mobli M, Maciejewski MW, Schuyler AD, Stern AS, Hoch JC. Sparse sampling methods in multidimensional NMR. *Phys Chem Chem Phys*. 2012; 14:10835. [PubMed: 22481242]
3. Hyberts SG, Arthanari H, Robson SA, Wagner G. Perspectives in magnetic resonance: NMR in the post-FFT era. *J Magn Reson*. 2014; 241:60. [PubMed: 24656081]
4. Hyberts SG, Robson SA, Wagner G. Exploring signal-to-noise ratio and sensitivity in non-uniformly sampled multi-dimensional NMR spectra. *J Biomol NMR*. 2013; 55:167. [PubMed: 23274692]
5. Matsuki Y, Konuma T, Fujiwara T, Sugase K. Boosting protein dynamics studies using quantitative nonuniform sampling NMR spectroscopy. *J Phys Chem B*. 2011; 115:13740. [PubMed: 21992609]
6. Mobli M, Hoch JC. Maximum entropy spectral reconstruction of non-uniformly sampled data. *Concepts Magn Reson, Part A*. 2008; 32:436.
7. Hyberts SG, Milbradt AG, Wagner AB, Arthanari H, Wagner G. Application of iterative soft thresholding for fast reconstruction of NMR data non-uniformly sampled with multidimensional Poisson Gap scheduling. *J Biomol NMR*. 2012; 52:315. [PubMed: 22331404]
8. Orekhov VY, Jaravine VA. Analysis of non-uniformly sampled spectra with multi-dimensional decomposition. *Prog Nucl Magn Reson Spectrosc*. 2011; 59:271. [PubMed: 21920222]
9. Hyberts SG, Heffron GJ, Tarragona NG, Solanky K, Edmonds KA, Luithardt H, Fejzo J, Chorev M, Aktas H, Colson K, Falchuk KH, Halperin JA, Wagner G. Ultrahigh-resolution (1)H-(13)C HSQC spectra of metabolite mixtures using nonlinear sampling and forward maximum entropy reconstruction. *J Am Chem Soc*. 2007; 129:5108. [PubMed: 17388596]
10. Hyberts SG, Frueh DP, Arthanari H, Wagner G. FM reconstruction of non-uniformly sampled protein NMR data at higher dimensions and optimization by distillation. *J Biomol NMR*. 2009; 45:283. [PubMed: 19705283]
11. Yoon JW, Godsill S, Kupce E, Freeman R. Deterministic and statistical methods for reconstructing multidimensional NMR spectra. *Magn Reson Chem*. 2006; 44:197. [PubMed: 16566032]
12. Kazimierczuk K, Orekhov VY. Accelerated NMR spectroscopy by using compressed sensing. *Angew Chem Int Ed*. 2011; 50:5556.



13. Holland DJ, Bostock MJ, Gladden LF, Nietlispach D. Fast multidimensional NMR spectroscopy using compressed sensing. *Angew Chem Int Ed*. 2011; 50:6548.
14. Shrot Y, Frydman L. Compressed sensing and the reconstruction of ultrafast 2D NMR data: Principles and biomolecular applications. *J Magn Reson*. 2011; 209:352. [PubMed: 21316276]
15. Matsuki Y, Eddy MT, Herzfeld J. Spectroscopy by integration of frequency and time domain information for fast acquisition of high-resolution dark spectra. *J Am Chem Soc*. 2009; 131:4648. [PubMed: 19284727]
16. Matsuki Y, Eddy MT, Griffin RG, Herzfeld J. Rapid three-dimensional MAS NMR spectroscopy at critical sensitivity. *Angew Chem Int Ed*. 2010; 49:9215.
17. Coggins BE, Zhou P. High resolution 4-D spectroscopy with sparse concentric shell sampling and FFT-CLEAN. *J Biomol NMR*. 2008; 42:225. [PubMed: 18853260]
18. Kazimierczuk K, Zawadzka A, Kořmi ski W. Optimization of random time domain sampling in multidimensional NMR. *J Magn Reson*. 2008; 192:123. [PubMed: 18308599]
19. Barna JCJ, Laue ED, Mayger MR, Skilling J, Worrall SJP. Exponential sampling, an alternative method for sampling in two-dimensional NMR experiments. *J Magn Reson*. 1987; 73:69.
20. Kazimierczuk K, Zawadzka A, Kořmi ski W. Narrow peaks and high dimensionalities: exploiting the advantages of random sampling. *J Magn Reson*. 2009; 197:219. [PubMed: 19185522]
21. Kazimierczuk K, Stanek J, Zawadzka-Kazimierczuk A, Kořmi ski W. Random sampling in multidimensional NMR spectroscopy. *Prog Nucl Magn Reson Spectrosc*. 2010; 57:420. [PubMed: 20920758]
22. Hoch JC, Maciejewski MW, Filipovic B. Randomization improves sparse sampling in multidimensional NMR. *J Magn Reson*. 2008; 193:317. [PubMed: 18547850]
23. Kazimierczuk K, Zawadzka A, Kořmi ski W, Zhukov I. Lineshapes and artifacts in multidimensional Fourier transform of arbitrary sampled NMR data sets. *J Magn Reson*. 2007; 188:344. [PubMed: 17822933]
24. Hyberts SG, Takeuchi K, Wagner G. Poisson-gap sampling and forward maximum entropy reconstruction for enhancing the resolution and sensitivity of protein NMR data. *J Am Chem Soc*. 2010; 132:2145. [PubMed: 20121194]
25. Eddy MT, Ruben D, Griffin RG, Herzfeld J. Deterministic schedules for robust and reproducible non-uniform sampling in multidimensional NMR. *J Magn Reson*. 2012; 214:296. [PubMed: 22200565]
26. Schuyler AD, Maciejewski MW, Arthanari H, Hoch JC. Knowledge-based nonuniform sampling in multidimensional NMR. *J Biomol NMR*. 2011; 50:247. [PubMed: 21626215]
27. Kazimierczuk K, Orekhov VY. A comparison of convex and non-convex compressed sensing applied to multidimensional NMR. *J Magn Reson*. 2012; 223:1. [PubMed: 22960668]
28. Delaglio F, Grzesiek S, Vuister GW, Zhu G, Pfeifer J, Bax A. NMRPipe: a multidimensional spectral processing system based on UNIX pipes. *J Biomol NMR*. 1995; 6:277. [PubMed: 8520220]
29. Lustig M, Donoho D, Pauly JM. Sparse MRI: The application of compressed sensing for rapid MR imaging. *Magn Reson Med*. 2007; 58:1182. [PubMed: 17969013]
30. Maciejewski, MW. Schedule Tool. [http://sbtools.uchc.edu/nmr/sample\\_scheduler](http://sbtools.uchc.edu/nmr/sample_scheduler)
31. Johnson BA, Blevins RA. NMR View: a computer program for the visualization and analysis of NMR data. *J Biomol NMR*. 1994; 4:603. [PubMed: 22911360]

## Appendix A. Supplementary material

Supplementary figures and details of the methods used to generate sampling schemes and to reconstruct the spectra are given in the supporting information.

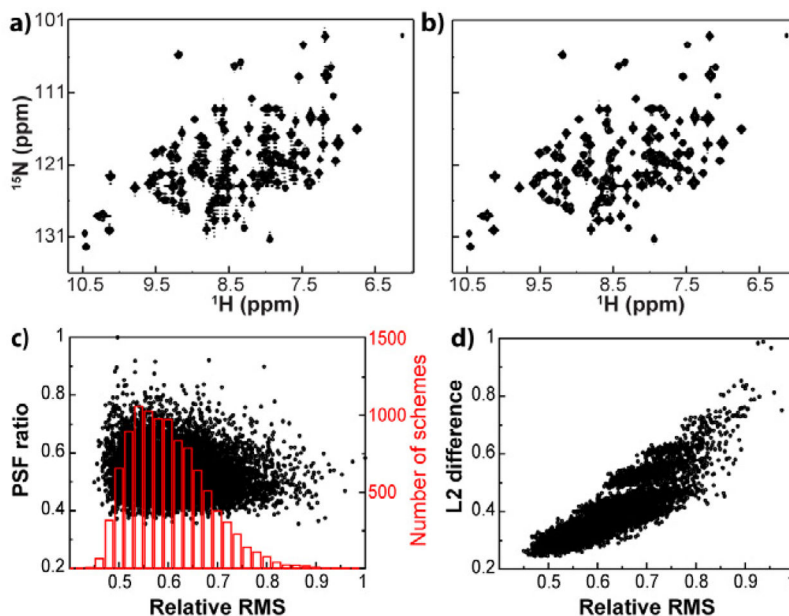


**Figure 1.**

Comparison of NUS schedules and currently used scoring methods. The (a) worst and (b) best reconstruction based on RMS for identically processed synthetic data containing no noise. (c) The PSF ratio (max side-lobe:zero frequency peak) of the sampling scheme does not accurately predict artifacts in reconstructed spectra (black circles). The number of NUS schedules that result in a given reconstruction RMS is shown in red. (d) The  $l_2$  norm, or the non-normalized root mean squared difference between a linearly sampled synthetic spectrum and the NUS spectrum, is able to predict artifacts in other spectra sampled with the same NUS schemes (black circles).



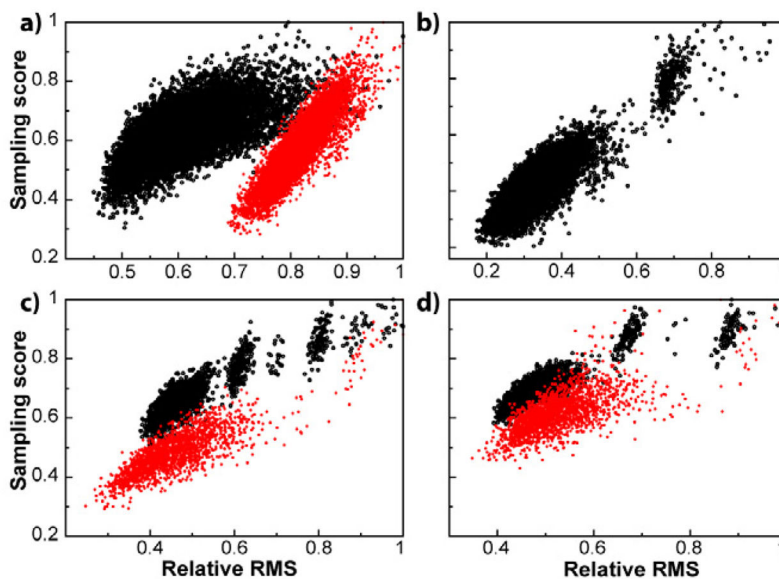


**Figure 2.**

Empirically derived NUS scoring function obtained with synthetic data. (a) The same synthetic data and schemes used in Figure 1 were analyzed with the NUS scoring function. A correlation coefficient,  $\rho$ , of 0.66 was found between RMS and the NUS score when spectra were reconstructed using compressed sensing (black). The correlation coefficient of DFT spectra was found to be  $\rho = 0.88$  (red). (b) Synthetic spectra with linewidths similar to a  $^{13}\text{C}$  methyl HSQC were used to test the generality of the scoring function. A correlation coefficient,  $\rho$ , of 0.77 was found with compressed sensing reconstruction. (c) Sampling scores for 30% (60%) NUS of 256 linear increments in black (red). The correlation coefficient for scores and RMS for 30% (60%) NUS was found to be  $\rho = 0.75$  (0.87). (d) Sampling scores for 30% (60%) of 512 linear increments in black (red) have a correlation coefficient of  $\rho = 0.71$  (0.62).

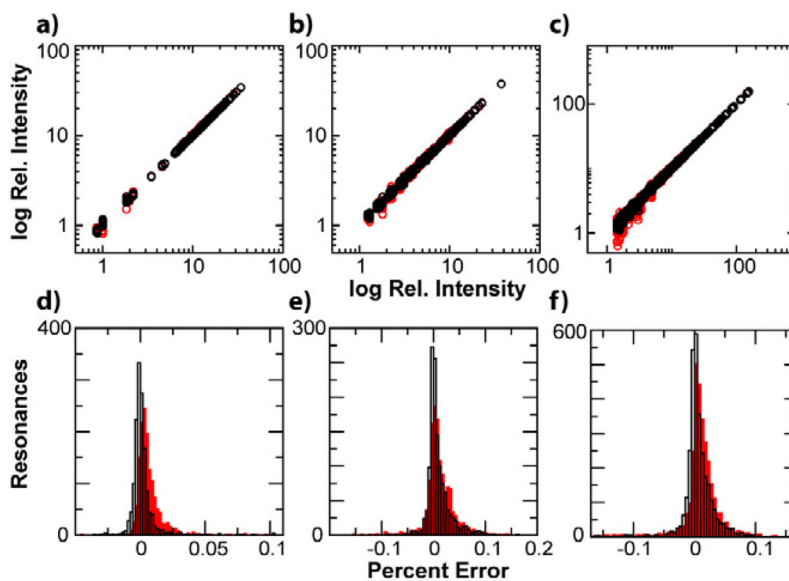


**Figure 3.** Intensities derived from reconstructed NUS data at 60% sampling. Correlation between cross peak intensities resulting from reconstruction of NUS data versus intensities in uniformly sampled spectrum for the 10 best(worst) sampling schemes in black(red) for  $^1\text{H}$ - $^{15}\text{N}$  HSQC/TROSY spectra of (a) DHFR, (b) apoMb, and (c) p38 $\gamma$ . The percent error in intensity reconstruction for the 10 best(worst) scored schemes for resonance cross-peaks in black(red) of (d) DHFR, (e) apoMb, and (f) p38 $\gamma$ .